



1     **Atmospheric fate of two relevant unsaturated ketoethers: kinetics, products and**  
2     **mechanisms for the reaction of hydroxyl radicals with (*E*)-4-methoxy-3-buten-2-**  
3     **one and 1-(*E*)-1-methoxy-2-methyl-1-penten-3-one.**

4     Rodrigo Gastón Gibilisco<sup>\*a</sup>, Ian Barnes<sup>a†</sup>, Iustinian Gabriel Bejan<sup>\*b</sup>, Peter Wiesen<sup>a</sup>

5

6     <sup>a</sup>*Bergische Universität Wuppertal, Institute for Atmospheric and Environmental*  
7     *Research, 42097 Wuppertal / Germany.*

8     <sup>b</sup>*Faculty of Chemistry and Integrated Center of Environmental Science Studies in the*  
9     *North East Region - CERNESIM, “Al. I. Cuza” University, Iasi, Romania*

10

11

12

13

14

15

16

17

18

19

20

21

22

23

24

25

26

27

28

29

30

31

32

33

34

35

36

37

38

39

40



1 **Abstract**

2 The kinetics of the gas-phase reactions of hydroxyl radicals with two unsaturated  
3 methoxy-ketones at  $(298 \pm 3)$  K and 1 atm of synthetic air have been studied for the first  
4 time using the relative rate technique in an environmental reaction chamber by in situ  
5 FTIR spectrometry. The rate coefficients obtained using propene and isobutene as  
6 reference compounds were (in units of  $10^{-10} \text{ cm}^3 \text{ molecule}^{-1} \text{ s}^{-1}$ ) as follows:  $k_1(\text{OH} + (E)$   
7  $4\text{-methoxy-3-buten-2-one}) = (1.42 \pm 0.12)$ , and  $k_2(\text{OH} + 1\text{-}(E)\text{-1-methoxy-2-methyl-1-}$   
8  $\text{penten-3-one}) = (3.34 \pm 0.43)$ . In addition, quantification of the main oxidation products  
9 has been performed and degradation mechanisms for these reactions were developed. The  
10 formation products and kinetic data confirm that the reactions proceed mainly via an  
11 addition of the OH radical to the double bond. Gas phase products, identified and  
12 quantified from these reactions, are carbonyls like methyl formate, methyl glyoxal and  
13 2,3-pentanedione and long-lived nitrogen containing compounds such as PAN and PPN.  
14 Atmospheric lifetimes and the ozone formation potential have been estimated and  
15 possible atmospheric implications assessed.

16  
17 *Keywords:*  $(E)$ -4-methoxy-3-buten-2-one, 1- $(E)$ -1-methoxy-2-methyl-1-penten-3-one,  
18 OH radical kinetic, tropospheric chemistry, gas phase degradation mechanism, biomass  
19 burning, PAN and carbonyl formation.

20 \* Corresponding authors.

21 *E-mail address:*

22 gibilisco@uni-wuppertal.de (R. G. Gibilisco)

23 iustinian.bejan@uaic.ro (I. Bejan)

24 † Deceased 1 January 2018

25

26



1 **1. Introduction**

2 Oxygenated volatile organic compounds (OVOCs) are ubiquitous atmospheric  
3 constituents of anthropogenic and natural origin. From those OVOCs, carbonyls have  
4 both direct and indirect sources, as a result of biogenic and anthropogenic activities, and  
5 because they are formed during chemical degradation processes, which occur in the  
6 atmosphere. Unsaturated carbonyls present high reactivity and are easily decomposed  
7 throughout chemical reactions into various OVOCs products.

8 Ketones are one of the dominant groups of carbonyls found in the lower troposphere.  
9 They can be emitted into the atmosphere by anthropogenic activities from industry,  
10 combustion engine vehicle exhaust and in a large extent are formed as reaction products  
11 of other VOCs in the troposphere (Calvert et al., 2011; Jiménez et al., 2014; Mellouki et  
12 al., 2015).

13 More complex unsaturated carbonyls, namely the  $\alpha$ ,  $\beta$ -unsaturated ketones and  $\alpha$ ,  $\beta$ -  
14 unsaturated ethers are either emitted by plants or are produced as a result of atmospheric  
15 oxidation of conjugated dienes (Lv et al., 2018; Mellouki et al., 2015; Zhou et al., 2006).  
16 These compounds have been considered as precursors for secondary organic aerosols  
17 (SOA) (Calvert et al., 2011).

18  $\alpha$ ,  $\beta$ -unsaturated keto ethers (UKE) are higher structural complexity compounds found in  
19 the atmosphere. They were detected as products during gas phase atmospheric  
20 degradation of furans and unsaturated ethers, compounds, which received substantial  
21 interest in the last decade since they are considered promising alternative fuels (Cilek et  
22 al., 2011; Li et al., 2018; Villanueva et al., 2009; Zhou et al., 2006). UKE compounds are  
23 produced during combustion and more specifically biomass burning events (Hatch et al.,  
24 2015). They are also of great interest in the pharmaceutical industry since they are often



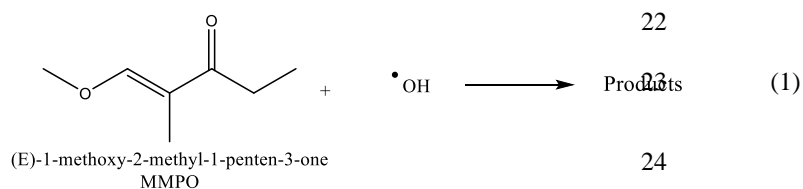
1 used as precursors and/or intermediates in the production of new anticancer drugs (Gøgsig  
2 et al., 2012; Kumar et al., 2016).

3 It is known that the oxidative chemistry of VOCs in the troposphere is governed mainly  
4 by the reaction with hydroxyl radicals (OH) either by addition to a C-C double bond or  
5 by abstraction of hydrogen atoms from the molecule.  $\alpha$ ,  $\beta$ -unsaturated keto ethers are a  
6 special type of olefins, with an electron rich  $\pi$  system, which makes them more  
7 susceptible to rapid oxidation by addition of the OH radical to the double bond. Secondary  
8 pollutants, which are formed in such a reaction sequence could be even more harmful  
9 than primary pollutants emitted into the atmosphere. Examples of such secondary harmful  
10 pollutants are ozone, organic peroxy nitrates, in urban areas with high concentrations of  
11 nitrogen oxides,  $\text{NO}_x$ , highly oxidized molecules (HOM) and/or secondary organic  
12 aerosols (Atkinson, 2000; Calvert, J.G., Orlando, J.J., Stockwell, W.R. and Wallington,  
13 2015).

14 Accordingly, it is important to study in detail how the OH radical initiated oxidation of  
15 these compounds can affect the chemical composition and reactivity of the troposphere  
16 and, furthermore, the impact of the secondary pollutants formed during their gas phase  
17 chemical degradation.

18 In the present work the OH radical initiated reactions of (*E*)-1-methoxy-2-methyl-1-  
19 penten-3-one (MMPO) and (*E*)-4-methoxy-3-buten-2-one (TMBO) have been  
20 investigated:

21

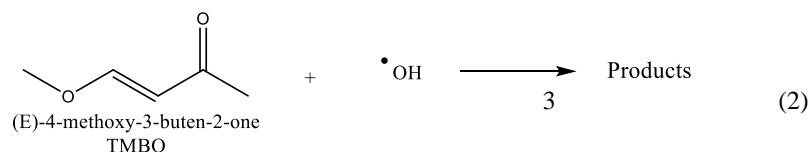


25



1

2



4

5 In addition to the kinetic information, products have been quantified and reaction  
6 mechanisms have been derived for both compounds.

7 The present study represents the first experimental determination of the rate coefficients  
8 ( $k_{OH}$ ) and the reaction products formed from the gas phase reactions in the presence of  
9 NO. The obtained results could be used to generate more complete atmospheric chemical  
10 degradation mechanisms, i.e. the master chemical mechanism, which are necessary for a  
11 better estimation of the contribution of such compounds to photooxidant and SOA  
12 formation.

13

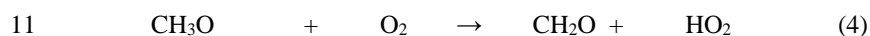
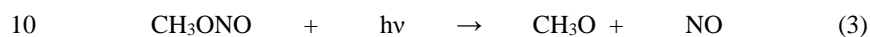
## 14 2. Experimental

15 All experiments were performed in a 1080 L quartz-glass reaction chamber at  $(298 \pm 3)$   
16 K and a total pressure of  $(760 \pm 10)$  Torr of synthetic air. A pumping system consisting  
17 of a turbo-molecular pump backed by a double stage rotary fore pump was used to  
18 evacuate the reactor to  $10^{-3}$  Torr. Three magnetically coupled Teflon mixing fans are  
19 mounted inside the chamber to ensure homogeneous mixing of the reactants. The  
20 photolysis system consists of 32 superactinic fluorescent lamps (Philips TL05 40W: 290–  
21 480 nm,  $\lambda_{\text{max}} = 360$  nm) and 32 low-pressure mercury vapor lamps (Philips TUV 40W;  
22  $\lambda_{\text{max}} = 254$  nm), which are spaced evenly around the reaction vessel. The lamps are wired  
23 in parallel and can be switched individually, which allows variation of the light intensity,  
24 and thus also the photolysis frequency/radical production rate, within the chamber. The



1 chamber is equipped with a White type multiple-reflection mirror system with a base  
2 length of  $(5.91 \pm 0.01)$  m for sensitive in situ long path infrared absorption monitoring of  
3 reactants and products in the spectral range  $4000 - 700 \text{ cm}^{-1}$ . The White system was  
4 operated at 82 traverses, giving a total optical path length of  $(484.7 \pm 0.8)$  m. Infrared  
5 spectra were recorded with a spectral resolution of  $1 \text{ cm}^{-1}$  using a Nicolet Nexus FT-IR  
6 spectrometer equipped with a liquid nitrogen cooled mercury-cadmium-telluride (MCT)  
7 detector.

8 OH radicals were generated by photolysis of  $\text{CH}_3\text{ONO}/\text{NO}/\text{air}$  mixtures at 360 nm using  
9 fluorescent lamps:



13

14 Quantification of reactants and products was performed by comparison with calibrated  
15 reference spectra contained in the IR spectral data bases of the Wuppertal laboratory.

16 To investigate the mechanism of the OH-radical initiated oxidation of the  $\alpha$ ,  
17  $\beta$ -unsaturated keto ethers, the mixtures of the compound,  $\text{CH}_3\text{ONO}/\text{NO}$  and air were  
18 irradiated for periods of 10-30 minutes during which infrared spectra were recorded with  
19 the FTIR spectrometer. Typically, 64 interferograms were co-added per spectrum over a  
20 period of approximately 1 min and 15-20 such spectra were collected.

21 The reactants were monitored at the following infrared absorption frequencies (in  $\text{cm}^{-1}$ ):  
22 TMBO at 958, 1253 and 3020, MMPO at 1245, 1653 and 2850, isobutene at 3085 and  
23 propene at 3091.



1 Rate coefficients for the reactions of OH radicals with MMPO and TMBO were  
2 determined by comparing their decay rate with that of the corresponding decay of the two  
3 reference compounds, isobutene and propene:



6 Provided that the reference compound and the reactants are lost only by reactions (6) and  
7 (7), it can be shown that:

8 
$$\ln \left\{ \frac{[\text{UKE}]_0}{[\text{UKE}]_t} \right\} = \frac{k_6}{k_7} \ln \left\{ \frac{[\text{reference}]_0}{[\text{reference}]_t} \right\} \quad (\text{I})$$

9 where,  $[\text{UKE}]_0$ ,  $[\text{reference}]_0$ ,  $[\text{UKE}]_t$  and  $[\text{reference}]_t$  are the concentrations of the  $\alpha$ ,  $\beta$ -  
10 unsaturated keto ethers and the reference compound at times  $t=0$  and  $t$ , respectively, and  
11  $k_6$  and  $k_7$  are the rate coefficients of reactions (6) and (7), respectively.

12 The initial mixing ratios of the reactants in ppmV ( $1 \text{ ppmV} = 2.46 \times 10^{13} \text{ molecule cm}^{-3}$   
13 at 298 K and 1 atm) were TMBO (1-3), MMPO (2-4), isobutene (3-5) and propene (3-5).

14 Possible additional losses due to interferences and/or interactions with the reactor walls  
15 could be neglected or corrected. To verify this assumption, mixtures of  $\text{CH}_3\text{ONO}/\text{NO}/\text{air}$   
16 with the  $\alpha$ ,  $\beta$ -unsaturated keto ethers and the reference compound were prepared and  
17 allowed to stand in the dark for two hours. In all cases, the decay of the organic species  
18 in the presence of the OH radical precursor and in the absence of UV light was negligible.  
19 Furthermore, to test for a possible photolysis of the compounds, the reactant mixtures  
20 without OH radical precursor were irradiated for 30 minutes, using all lamps surrounding  
21 the chamber. No significant photolysis of any of the reactants was observed and no  
22 additional decay has been monitored due to a possible reaction with interfering radicals.

23  
24  
25



### 1        3. Materials

2        The following chemicals, with purities as stated by the supplier, were used without further  
3        purification: synthetic air (Air Liquide, 99.999%), propene (Messer Schweiz AG, 99.5%),  
4        isobutene (Messer, 99%), (*E*)-4-methoxy-3-buten-2-one technical grade (Aldrich, 90%)  
5        and 1-(*E*)-1-methoxy-2-methyl-1-penten-3-one (Aldrich, > 89.5 %). Methyl nitrite was  
6        prepared by the drop-wise addition of 50% sulfuric acid to a saturated solution of sodium  
7        nitrite in water and methanol (Taylor et al., 1980). The products were carried by a stream  
8        of nitrogen gas through a saturated solution of sodium hydroxide followed by calcium  
9        chloride, to remove excess acid, water and methanol, respectively. Methyl nitrite was  
10       collected and stored at 193 K in dry ice.

11

### 12        4. Results and Discussion

#### 13        4.1 Rate coefficients for the reaction with OH radicals

14       Plots of the kinetic data obtained from the experiments of the reaction of OH radicals with  
15       TMBO and MMPO using two different reference compounds are shown in Fig. 1 and 2,  
16       respectively. At least two experiments have been performed for each reference compound  
17       and linear plots were obtained in all cases. For better representation, data for all  
18       experiments have been plotted against both references. Rate coefficient ratio  
19        $k_{\text{UKE}}/k_{\text{Reference}} (\pm 2\sigma)$  obtained by combining the experiments results in Fig. 1 and Fig. 2  
20       were: for TMBO,  $k_{\text{TMBO}}/k_{\text{isobutene}} = (2.56 \pm 0.13)$  and  $k_{\text{TMBO}}/k_{\text{propene}} = (5.08 \pm 0.16)$ . For  
21       MMPO,  $k_{\text{MMPO}}/k_{\text{isobutene}} = (6.40 \pm 0.31)$  and  $k_{\text{MMPO}}/k_{\text{propene}} = (11.64 \pm 0.82)$ .

22       The linearity of the plots with near-zero intercepts confirms that no interferences have  
23       affected the rate coefficient determination. Additionally, the very good agreement of the  
24       rate coefficients using the two reference compounds proved the correctness of the  
25       investigations.



1 Table 1 lists the values of the rate coefficient ratio  $k_{UKE}/k_{reference}$  obtained in the  
2 individual experiments at 298 K and 1 atm for each  $\alpha$ ,  $\beta$ -unsaturated keto ether. The  
3 errors given for the  $k_{UKE}/k_{reference}$  ratios are the  $2\sigma$  statistical errors from the linear  
4 regression. The rate coefficients  $k_{OH}$  for reactions 1 and 2 were calculated using the  
5 recommended values  $k = (2.90 \pm 0.10) \times 10^{-11} \text{ cm}^3 \text{ molecule}^{-1} \text{ s}^{-1}$  (Atkinson et al., 2006)  
6 (OH + propene) and  $k = (5.23 \pm 0.24) \times 10^{-11} \text{ cm}^3 \text{ molecule}^{-1} \text{ s}^{-1}$  (OH + isobutene)  
7 (Atkinson and Aschmann, 1984).

8 In addition, Table 1 shows the rate coefficients for individual experiments of each  
9 reference compound employed in this study as well as the final quoted rate coefficients  
10 for the reactions of OH with UKE compounds as an average from all experimental values  
11 obtained for the corresponding compound. The error quoted for those final UKE rate  
12 coefficients are obtained by using an error propagation approach.

13 To the best of our knowledge rate coefficients for the reactions of OH radicals with (*E*)-  
14 4-methoxy-3-buten-2-one and 1-(*E*)-1-methoxy-2-methyl-1-penten-3-one have not been  
15 reported previously in the literature.

16

#### 17 4.1.1 Reactivity trends

18 There is a general lack of studies on the reactivity of poly-substituted oxygenated  
19 unsaturated compounds, such as the unsaturated keto ethers studied in this work.

20 Only the reactivity of (*E*)-4-methoxy-3-buten-2-one towards ozone was investigated by  
21 Grosjean and Grosjean (1999) who reported a rate coefficient  $k_{O_3}$  of  $1.3 \times 10^{-16} \text{ cm}^3$   
22  $\text{molecule}^{-1} \text{ s}^{-1}$  (Grosjean and Grosjean, 1999). The authors identified and quantified two  
23 main products from the ozonolysis of (*E*)-4-methoxy-3-buten-2-one, namely  
24 methylglyoxal ( $31.2 \pm 1.9\%$ ) and methyl formate ( $> 15.7\%$ ). These two species are  
25 potential products of the OH-initiated oxidation of (*E*)-4-methoxy-3-buten-2-one as well.



1 It is well known that OH-initiated atmospheric degradation of unsaturated VOCs  
2 proceeds mainly through the addition of the OH radical to the double bond (Calvert et al.,  
3 2015). Some studies also suggested that the presence of oxygenated functional groups in  
4 unsaturated VOCs leads to an increase of  $k_{OH}$ , perhaps due to the possibility of hydrogen  
5 bonding transition complexes stabilizing the transition states involved in these reactions  
6 (Blanco et al., 2012; Gaona-Colmán et al., 2017; Mellouki et al., 2003).

7 Considering the findings mentioned above, it is interesting to analyze the possible effect  
8 on  $k_{OH}$  when the ether group (R-O-R') is directly attached to the C=C bond of the  
9 unsaturated ketones and the presence of different substituent in the molecule. For this  
10 purpose, Table 2 present two basic structures of unsaturated ketones (I and II) and the OH  
11 rate coefficients for different unsaturated ketones obtained experimentally and/or  
12 estimated using a SAR method (US EPA. Estimation Programs Interface Suite™ for  
13 Microsoft® Windows, 2018).

14 Starting with the less substituted compound, when the substituents  $R_1$ ,  $R_2$ , and  $R_3$  are all  
15 hydrogen atoms (3-buten-2-one), a value of  $k_{OH} = 2 \times 10^{-11} \text{ cm}^3 \text{ molecule}^{-1} \text{ s}^{-1}$  was  
16 experimentally observed (Holloway et al., 2005). Successive replacement of H atoms  
17 with methyl groups, for the positions  $R_2$  (3-penten-2-one) and  $R_3$  (4-methyl-3-penten-2-  
18 one), leads to a considerable increment on the reactivity as shown in Table 2 (Blanco et  
19 al., 2012; Gaona-Colmán et al., 2017). Considering the experimental errors of the  
20 measurements it is reasonable to conclude that the addition of each methyl group leads to  
21 an increase of approximately  $4 \times 10^{-11} \text{ cm}^3 \text{ molecule}^{-1} \text{ s}^{-1}$  in the rate coefficient relative  
22 to those of basic structure I.

23 The methyl group added in positions  $R_2$  and  $R_3$  would stabilize the radical formed after  
24 the addition of the OH at the  $C_\alpha$  for two different effects: (i) the positive inductive effect



1 (I+) by the methyl group, which stabilizes the positive charge in the  $C_{\beta}$  atom and (ii) the  
2 stabilization due to the hyperconjugation of the carbocation formed at the  $C_{\beta}$ .  
3 Comparing the experimental value  $k_{OH} = 1.42 \times 10^{-10} \text{cm}^3 \text{ molecule}^{-1} \text{s}^{-1}$  obtained in the  
4 present work for (*E*)-4-methoxy-3-buten-2-one with its methylated analogue 3-penten-2-  
5 one, one can easily realize the increase by a factor of 2 in the rate coefficient when the  $R_3$   
6 substituent is a methoxy group. This can be explained by the oxygen's lone pair of  
7 electrons, which delocalizes and increases electron density within the C=C bond. On the  
8 other hand, the methoxy group is electron deducting through a negative inductive effect  
9 (I-) via the  $\sigma$  bonds. However, the mesomeric effect is stronger than the inductive one,  
10 which is reflected by an increase of the (*E*)-4-methoxy-3-buten-2-one + OH reaction rate  
11 coefficient compared to its mono and bi-methylated analogues that can stabilize the  
12 corresponding radical structures only by the inductive effect and hyperconjugation, but  
13 not by a mesomeric effect.

14 A similar assessment can be performed considering the basic structure (II). The increasing  
15 trend in the reactivity towards OH radicals is quite similar when methyl groups replace H  
16 atoms in the structure of 1-pentene-3-one. The experimental rate coefficient of  $3.34 \times 10^{-10}$   
17  $\text{cm}^3 \text{ molecule}^{-1} \text{s}^{-1}$  obtained in the present work for the reaction of OH radicals with (*E*)-  
18 1-methoxy-2-methyl-1-penten-3-one is quite high but considering the approximate  
19 individual contribution of the substituents on the C=C bond as it was assumed previously  
20 for the basic structure (I) reflects entirely the system reactivity.

21

#### 22 4.1.2 Structure-activity relationship (SAR) calculations

23 In the present work, the AOPWIN software included in the EpiSuite 4.1 was used to  
24 estimate the rate coefficients of the structures listed in Table 2 (US EPA. Estimation  
25 Programs Interface Suite™ for Microsoft® Windows, 2018).



1 It is worth mentioning that calculated  $k_{OH}$  with AOPWIN fit quite well with the  
2 experimental values of the simplest structures of the unsaturated ketones shown in Table  
3 2, namely 3-buten-2-one and 1-penten-3-one. However, when the hydrogen atoms are  
4 replaced by methyl groups in the C=C system for structures (I) and (II), differences  
5 between experimental values and those estimated using SAR method become evident by  
6 a factor of 1.2 and 1.5, respectively. For structure (I) with two methyl substituents (4-  
7 methyl-3-penten-2-one) the difference remains approximately the same (factor 1.3).  
8 Comparing the kinetic results obtained in this work for MMPO and TMBO with those  
9 predicted by AOPWIN, the differences become substantially larger. In Table 2 it can be  
10 seen that for TMBO the results differ by a factor of two and for MMPO by a factor of  
11 three.  
12 This fact highlights the limitations of the AOPWIN-SAR method for predicting the  
13 specific site for the addition of the OH radical to each carbon atom of an asymmetrical  
14 alkene, ignoring a possible stabilization of the reaction intermediate. The stabilization  
15 could generate transition states involving the formation of hydrogen bonding complexes  
16 between the OH radical and the oxygenated substituents as it was suggested in previous  
17 publications (Blanco et al., 2012; Gaona-Colmán et al., 2017; Mellouki et al., 2003).  
18 In conclusion, the AOPWIN-SAR estimation of reaction rate coefficients is a useful tool  
19 for simple molecules. However, the OH rate coefficients of the unsaturated keto-ethers  
20 reported in this work showed significant discrepancies compared with the predicted ones.  
21 Probably, as suggested recently by Vereecken et al.(2018) it is not clear if the SAR  
22 method can be easily expanded to multifunctional compounds, especially given the small  
23 training set available from which to derive cross-substituent parameters or base rate  
24 coefficients (Vereecken et al., 2018).

25



1    4.2 Mechanism and product distribution

2    It is well known that reactions of unsaturated compounds will proceed mainly by initial  
3    addition of OH to the C=C bond leading to the formation of two  $\beta$ -hydroxyalkyl radicals,  
4    which in turn rapidly react with oxygen forming  $\beta$ -hydroxyalkyl peroxy radicals  
5    (Atkinson, 2007). Besides the addition pathway, H-atom abstraction also can occur in the  
6    reaction system. However, based on the structure reactivity relationships presented in  
7    table 2, this is expected to contribute no more than 2% to the overall reactivity.

8    In the presence of NO and O<sub>2</sub>, the peroxy radicals formed in the first step of the reaction  
9    could react further to form mainly 1,2-hydroxyalkoxy radicals. These radicals, once being  
10   formed, can decompose and/or isomerize. Based on experimental evidence and identified  
11   reaction products performed in the present study, the potential reactions of the alkoxy  
12   radicals and the reaction sequence described above are shown in the generalized Schemes  
13   1 and 2 for each compound studied in the present work.

14

15   4.2.1 (*E*)-4-methoxy-3-buten-2-one + OH radicals

16   Figure 3 shows an IR spectrum recorded before (trace A) UV irradiation applied for a  
17   mixture of (*E*)-4-methoxy-3-buten-2-one (TMBO) and CH<sub>3</sub>ONO/NO in air. Trace B  
18   shows the spectrum recorded after 10 min of UV irradiation of the reaction mixture. Trace  
19   D exhibits the product spectrum after subtraction of not reacted TMBO (from the  
20   reference spectra trace C), NO, NO<sub>2</sub>, CH<sub>3</sub>ONO and H<sub>2</sub>O. Traces E, F and G show  
21   reference spectra of methyl formate, peroxyacetyl nitrate (PAN) and methyl glyoxal,  
22   respectively. Trace H exhibits the residual product spectrum that is obtained after  
23   subtraction of known products from the product spectrum in trace D. The absorption from  
24   CO<sub>2</sub> has been removed in all traces for clarity since the band was saturated and no  
25   information could be obtained from it accordingly. Methyl formate, peroxyacetyl nitrate,



1 and methyl glyoxal were readily identifiable as reaction products. Concentration–time  
2 profiles of TMBO and the identified products, methyl formate, PAN, and methyl glyoxal  
3 are shown in Fig. 4. The concentration–time distribution supports that methyl formate,  
4 methyl glyoxal and PAN are primary reaction products.

5 Depending on the side addition of the OH radical leading to the  $C_\alpha$  or  $C_\beta$ , hydroxyalkoxy  
6 radicals,  $A_1$  and  $B_1$  will be formed respectively (Scheme 1). Decomposition of the  $A_1$   
7 radical will lead to the formation of methyl formate and methyl glyoxal as primary  
8 products. On the other hand,  $C_3$ - $C_4$  bond scission in the  $B_1$  radical will lead to the  
9 formation of methyl formate and methyl glyoxal. Additionally, the radical  $B_1$  could  
10 decompose through a  $C_2$ - $C_3$  scission generating 2-hydroxy-2-methoxyacetaldehyde and  
11 the acetyl radical. This route would, beside the formation of 2-hydroxy-2-  
12 methoxyacetaldehyde, be responsible for the primary generation of PAN through further  
13 reaction of the acetyl radical with  $O_2/NO_2$ . In addition, PAN is known to be formed due  
14 to the oxidation of methyl glyoxal (Fischer et al., 2014). The reaction of OH radicals with  
15 methyl glyoxal occurs exclusively by abstraction of the aldehydic H-atom to form  
16  $CH_3C(O)CO$  radicals, which have a very short lifetime, dissociating to form  $CH_3CO +$   
17  $CO$  (Green et al., 1990). Finally, it is expected that acetyl radicals react, in the presence  
18 of  $O_2$ , with  $NO_2$  to form PAN (Fischer et al., 2014). Acetyl radicals are of particular  
19 importance in atmospheric chemistry as they are key contributors to important pollutants  
20 in the atmosphere. PAN (peroxyacetyl nitrate), in high  $NO_x$  environments, is formed  
21 exclusively from acetyl peroxy radicals in the presence of  $NO_x$ . However, in low  $NO_x$   
22 environments, acetyl radicals, in the presence of oxygen, generates acetyl peroxy radicals,  
23 which further reacts with  $HO_2$  radicals producing  $CH_3C(O)OOH$ ,  $CH_3C(O)OH$ ,  $O_3$  and  
24 OH radicals. These secondary products could have a high impact on the atmospheric  
25 chemistry on the global scale (Winiberg et al., 2016).



1 After subtraction of the identified products, the most prominent absorption feature in the  
2 IR residual spectra (Fig. 3 trace H) is a carbonyl band at  $1730\text{ cm}^{-1}$ , which is more  
3 characteristic for an aldehydic than a ketone absorption. This feature suggests the  
4 formation of 2-hydroxy-2-methoxyacetaldehyde, which is unfortunately not  
5 commercially available. Therefore, direct identification in the residual product spectrum  
6 is not possible by using a recorded IR reference spectrum.

7 Carbonyl absorptions in the IR spectra are present in the  $1600\text{-}1800\text{ cm}^{-1}$  range and 2-  
8 hydroxy-2-methoxyacetaldehyde identification in this region of the IR spectrum is not  
9 possible. Beside the parent compound, which is presenting features in this carbonyl  
10 absorption specific region, many other products formed during the reaction have  
11 absorptions in this range. All the products formed in the reaction system have a specific  
12 absorption in the carbonyl range (methyl glyoxal, methyl formate, PAN and 2-hydroxy-  
13 2-methoxyacetaldehyde). However, the later one must have an important pronounced  
14 peak in the O-H absorption area; therefore, we may assume the unique absorption at  $3550$   
15  $\text{cm}^{-1}$  as being attributed to the O-H absorption of 2-hydroxy-2-methoxyacetaldehyde (SI  
16 Fig. S1). This is a strong indication of the 2-hydroxy-2-methoxyacetaldehyde formation,  
17 which is in agreement with the proposed mechanism in Scheme 1.

18 Plots of the concentrations of the carbonyls formed vs reacted TMBO give molar  
19 formation yields of  $(65 \pm 12)\%$  for methyl formate,  $(56 \pm 16)\%$  for PAN and  $(69 \pm 14)$   
20  $\%$  for methyl glyoxal. The yields have been corrected for secondary reactions with OH  
21 radicals as well as for the photolysis and wall deposition processes where necessary  
22 (Tuazon et al., 1986). Exemplary plots for the product formation yields are shown in the  
23 SI Fig. S2.

24

25



1 4.2.2(*E*)-1-methoxy-2-methyl-1-penten-3-one + OH radicals

2 Figure 5, trace A shows the infrared spectrum for an initial reaction mixture of a (*E*)-1-  
3 methoxy-2-methyl-1-penten-3-one (MMPO)/CH<sub>3</sub>ONO/NO/air mixture prior to  
4 irradiation; trace B exhibits the spectrum recorded after 10 min of irradiation and hence  
5 the occurring reaction; trace C shows a reference spectrum of MMPO recorded in a  
6 separate experiment in air at 1atm and 298K; trace D shows the product spectrum  
7 recorded after 10 min of irradiation and after subtraction of not reacted MMPO as well as  
8 subtraction of CH<sub>3</sub>ONO, NO, H<sub>2</sub>O and NO<sub>2</sub> absorption bands; trace E shows a reference  
9 spectrum of methyl formate; trace F a reference spectrum of 2,3-pentanedione and trace  
10 G a reference spectrum of peroxypropionyl nitrate (PPN). Trace H shows the residual  
11 product spectrum after subtraction of the identified reaction products in trace D.

12 The absorption from CO<sub>2</sub> has been removed in all traces for clarity since the band was  
13 saturated and no additional information could be obtained, accordingly. Methyl formate  
14 and peroxypropionyl nitrate were identified as reaction products. Concentration–time  
15 profiles of MMPO, methyl formate and peroxypropionyl nitrate are shown in Fig. 6.  
16 Figure 6 supports that methyl formate and peroxypropionyl nitrate are primary reaction  
17 products.

18 After the addition of the OH radical to the double bond of MMPO and subsequent addition  
19 of an oxygen molecule followed by reaction with NO, two different hydroxyalkoxy  
20 radicals, A<sub>2</sub> and B<sub>2</sub> (scheme 2) could be generated. Unlike for TMBO, the reaction of  
21 MMPO with OH radicals at the C<sub>β</sub> position could lead to the formation of the more stable  
22 tertiary radical A<sub>2</sub> due to the presence of a methyl group in the α position to the carbonyl  
23 group.

24 Scheme 2 shows that both addition channels would lead to the formation of methyl  
25 formate and 2,3-pentanedione if the hydroxyalkoxy radical would follow dissociation of



1 bond I in the  $A_2$  radical intermediate and the dissociation of bond II in the  $B_2$  radical  
2 intermediate.

3 The hydroxyalkoxy radical  $B_2$  could lead, beside the formation of 2,3-pentanedione and  
4 methyl formate by following scission of bond II, to the formation of 2-hydroxy-2-methyl-  
5 3-oxopentanal as product and formaldehyde as reaction co-product as a result of the  
6 decomposition of the  $B_2$  radical from scission of bond I. Formaldehyde, could not be  
7 identified as reaction product since it is formed from  $CH_3ONO$  photolysis and is present  
8 in the reaction spectra. 2-hydroxy-2-methyl-3-oxopentanal is not commercially available  
9 and in the absence of a mass spectrometry technique, which could at least identify the  
10 mass of this product there is only an assumption of its formation.

11 Decomposition channel for the  $A_2$  radical could follow route I leading to the formation  
12 of 2,3-pentanedione and the radical  $CH_3OCHOH$ , which could further, in the presence of  
13 oxygen, form methyl formate as a co-product. Figure 5 trace E shows a reference  
14 spectrum of methyl formate. The absorption bands at  $1210\text{ cm}^{-1}$  and  $1755\text{ cm}^{-1}$  were used  
15 to identify and quantify the formation of methyl formate.

16 The formation of 2,3-pentanedione is confirmed qualitatively by comparison of the  
17 product spectrum (Fig. 5 trace D) with the existing reference spectrum (Fig. 5, trace F).  
18 Although there is no doubt in the formation of 2,3-pentanedione, the partial or total  
19 overlap of the low intensity absorption bands did not allow us to perform reliable  
20 subtraction results to proceed for its quantification. 2,3-pentanedione exists  
21 predominantly in the keto form with the enol form being present to a few percent, at the  
22 most, in the gas phase at room temperature (Kung, 1974; Szabó et al., 2011). The  
23 predominance of the keto form for this compound makes its reactivity in the reaction with  
24 OH radical much lower. Furthermore, in comparison with 2,4-pentanedione, a dicarbonyl  
25 compound having the enolic form predominantly and thus being more reactive toward



1 OH radicals ( $9.05 \times 10^{-11} \text{ cm}^3 \text{ molecule}^{-1} \text{ s}^{-1}$ ) (Zhou et al., 2008), 2,3-pentanedione, with a  
2 rate coefficient for the reaction with OH radicals of  $2.25 \times 10^{-12} \text{ cm}^3 \text{ molecule}^{-1} \text{ s}^{-1}$  (Szabó  
3 et al., 2011) is 40 times less reactive and consequently the secondary reaction with OH  
4 radicals could be of less importance (Messaadia et al., 2015).

5 On the other hand, photolysis quantum yields for 2,3-pentanedione using XeF laser  
6 radiation and UV lamps at room temperature in 1000 mbar of air were studied by Szabó  
7 et al., 2011. The results obtained in their work suggest that 2,3-pentanedione would suffer  
8 significant photochemical changes even at relatively long wavelengths involving short  
9 photolysis lifetime in the troposphere. If we consider these facts, it would be possible to  
10 expect a non-negligible photolysis of the compound in our experimental system under the  
11 conditions used for this study.

12 Decomposition of the A2 hydroxyalkoxy radical could follow the scission on route II  
13 leading to 1-hydroxy-1-methoxypropan-2-one and propionyl radical. 1-hydroxy-1-  
14 methoxypropan-2-one is not commercially available and thus is not possible to identify  
15 this compound by comparison with an infrared reference spectrum. However, the  
16 absorption band with the maximum at  $3512 \text{ cm}^{-1}$  could be assumed to the OH stretching  
17 band of 1-hydroxy-1-methoxypropan-2-one. (see SI Fig. S3). Fig. S3 apparently presents  
18 one main absorption attributed to O-H stretching band but because the more stable tertiary  
19 radical (A<sub>2</sub>) there it is possible that 1-hydroxy-1-methoxypropan-2-one is the compound  
20 responsible for this absorption in IR. The propionyl radical could further form  
21 peroxypropionyl nitrate (PPN) (Fig. 5 trace G) in the presence of O<sub>2</sub> and NO<sub>2</sub>.

22 Plots of the concentrations of methyl formate and PPN formed against reacted MMPO in  
23 the OH radical reaction give molar formation yields of  $(40 \pm 12) \%$  and  $(17 \pm 6) \%$   
24 respectively. The yields have been corrected for secondary reactions with OH radicals



1 using the method outlined by Tuazón et al., 1986. Exemplary plots of the product  
2 formation yields are shown in the SI Fig. S4.

3

#### 4 **5. Atmospheric Implications and Conclusions**

5 Once emitted into the atmosphere, it is expected that unsaturated keto-ethers such as  
6 TMBO and MMPO will follow gas phase degradation processes initiated by the main  
7 tropospheric oxidants (OH radicals, ozone, chlorine atoms and NO<sub>3</sub> radicals). Rate  
8 coefficients obtained in this work for the reaction of TMBO and MMPO with OH radicals  
9 were used to calculate their tropospheric lifetimes using the expression  $\tau_x=1/k_{ox}[Ox]$   
10 where [Ox] is the typical atmospheric concentration of the oxidant in the troposphere and  
11  $k_{ox}$  is the rate coefficient for the reaction of the TMBO and MMPO towards the oxidants.  
12 Considering 12-h day-time average OH radical concentration of  $2 \times 10^6$  molecule cm<sup>-3</sup>  
13 (global weighted-average concentration) (Bloss et al., 2005) an average lifetime of 0.98  
14 and 0.42 hours were estimated for TMBO and MMPO, respectively. As mentioned  
15 before, in the literature there is only one experimental determination for the TMBO  
16 reaction rate coefficient with O<sub>3</sub> performed by Grosjean et al. (1999). By using  $k_{O_3}=1.3 \times$   
17  $10^{-16}$  cm<sup>3</sup> molecule<sup>-1</sup> s<sup>-1</sup> and a 24-h average O<sub>3</sub> concentration of  $7 \times 10^{11}$  molecule cm<sup>-3</sup>  
18 (Logan, 1985) an estimated tropospheric residence time of 3.1 hours was calculated. A  
19 similar tropospheric lifetime is expected for MMPO towards ozone but due to the lack of  
20 kinetic data, no exact value could be calculated for MMPO. Unfortunately, no kinetic data  
21 are available for the reactions of TMBO and MMPO with Cl atoms and NO<sub>3</sub> radicals.  
22 However, it's possible reasonable to conclude that reaction with OH radicals is the main  
23 tropospheric removal pathway for the two keto ethers studied due to the short lifetimes  
24 calculated in this work. For ethers it is known that photodissociation quantum yields are  
25 relatively low and the photolysis of ketones becomes important only at high altitudes



1 (Mellouki et al., 2015). Thus, it is reasonable to assume that photolysis of the studied  
2 compounds is only of minor importance for their atmospheric removal.

3 The reaction products of the OH radical initiated degradation of MMPO and TMBO  
4 together with kinetic results obtained in this study, confirm that the main degradation  
5 mechanisms follow the addition pathways to the double bonds. Products, identified and  
6 quantified from these reactions, are carbonyls like methyl formate, methyl glyoxal and  
7 2,3-pentanedione and long-lived nitrogen containing compounds such as PAN and PPN.  
8 Both type of these oxygenated products could have further impact on atmospheric  
9 processes. The present study proposes new gas phase contributors to the total budget of  
10 methyl glyoxal in the atmosphere a well known precursor for SOA formation (Fu et al.,  
11 2008). Even more this study becomes important since MMPO and TMBO are VOCs  
12 possibly released from open biomass burning events whose emissions factors for methyl  
13 glyoxal are not well established (Zarzana et al., 2018). PAN and PPN, quantified also as  
14 reaction products, are phytotoxic air pollutants, which act as NO<sub>x</sub> reservoir in remote  
15 areas (Taylor, 1969). Beside a large number of PAN measurement campaigns, most recent  
16 chemical transport models still unsolved the PANs global distributions due to the lack of  
17 understanding of the PAN source attribution in the atmosphere (Fischer et al., 2014).  
18 Although the acetyl radical is intermediary in the formation of PAN in this study, by its  
19 acetyl peroxy radical formed in the presence of oxygen, this radical it could play an  
20 important role in the HO<sub>x</sub> balance over the low NO<sub>x</sub> environment. The acetyl peroxy  
21 radical is a well known precursor of OH radicals as a result of the reaction with HO<sub>2</sub> in  
22 the remote atmosphere (Winiberg et al., 2016). Therefore, the gas phase mechanism  
23 proposed in this study could be of importance for understanding atmospheric processes  
24 at the global scale, either in the atmosphere with low NO<sub>x</sub> levels or in the atmosphere



1 with increased NO<sub>x</sub>. The results of the present study provide improved insights regarding  
2 the important contribution of multifunctional VOCs in the chemistry of atmosphere.

3

#### 4 **6. Competing interests**

5 The authors declare that they have no conflict of interest.

6

#### 7 **7. Author contribution**

8 RG, IB, IGB, PW designed experimental setup, RG conducted the measurements, RG and  
9 IGB processed the data, RG, IGB and PW prepared the manuscript with contribution from  
10 all the co-authors on different stages of writing process.

11

#### 12 **8. Acknowledgements**

13 R. Gibilisco acknowledges the Alexander von Humboldt foundation for providing a  
14 Georg Forster postdoctoral fellowship. The authors acknowledge financial support from  
15 the European grant EUROCHAMP-2020 and the Deutsche Forschungsgemeinschaft  
16 (DFG). I. Bejan acknowledges the UEFISCDI grant PN-III-P4-ID-PCE-2016-0807.

17

#### 18 **9. References**

19 Atkinson, R.: Atmospheric chemistry of VOCs and NO(x), *Atmos. Environ.*, 34(12–14),  
20 2063–2101, doi:10.1016/S1352-2310(99)00460-4, 2000.

21 Atkinson, R. and Aschmann, S. M.: Rate constants for the reaction of OH radicals with  
22 a series of alkenes and dialkenes at 295 ± 1 K, *Int. J. Chem. Kinet.*, 16(10), 1175–1186,  
23 doi:10.1002/kin.550161002, 1984.

24 Atkinson, R., Baulch, D. L., Cox, R. A., Crowley, J. N., Hampson, R. F., Hynes, R. G.,  
25 Jenkin, M. E., Rossi, M. J. and Troe, J.: *Atmospheric Chemistry and Physics Evaluated*



- 1 kinetic and photochemical data for atmospheric chemistry: Volume II-gas phase  
2 reactions of organic species The IUPAC Subcommittee on Gas Kinetic Data Evaluation  
3 for Atmospheric Chemistry. [online] Available from: [www.atmos-chem-](http://www.atmos-chem-phys.net/6/3625/2006/)  
4 [phys.net/6/3625/2006/](http://www.atmos-chem-phys.net/6/3625/2006/) (Accessed 28 August 2019), 2006.
- 5 Blanco, M. B. and Teruel, M. A.: Atmospheric photodegradation of ethyl vinyl ketone  
6 and vinyl propionate initiated by OH radicals, *Chem. Phys. Lett.*, 502,(4–6), 159–162,  
7 doi:10.1016/j.cplett.2010.12.059, 2011.
- 8 Blanco, M. B., Barnes, I. and Wiesen, P.: Kinetic investigation of the OH radical and Cl  
9 atom initiated degradation of unsaturated ketones at atmospheric pressure and 298 K, *J.*  
10 *Phys. Chem. A*, 116(24), 6033–6040, doi:10.1021/jp2109972, 2012.
- 11 Bloss, W. J., Evans, M. J., Lee, J. D., Sommariva, R., Heard, D. E. and Pilling, M. J.:  
12 The oxidative capacity of the troposphere: Coupling of field measurements of OH and a  
13 global chemistry transport model, *Faraday Discuss.*, 130, 425–436,  
14 doi:10.1039/b419090d, 2005.
- 15 Calvert, J.G., Orlando, J.J., Stockwell, W.R. and Wallington, T. J.: *The Mechanisms of*  
16 *Reactions Influencing Atmospheric Ozone*, Oxford University Press., 2015.
- 17 Calvert, J., Mellouki, A., Orlando, J. J., Pilling, M. J. . and Wallington, T. J.: *The*  
18 *Mechanisms of Atmospheric Oxidation of the Oxygenates*, Oxford University Press,  
19 New York., 2011.
- 20 Cilek, J. E., Ikediobi, C. O., Hallmon, C. F., Johnson, R., Onyeozili, E. N., Farah, S. M.,  
21 Mazu, T., Latinwo, L. M., Ayuk-Takem, L. and Berniers, U. R.: Semi-field evaluation  
22 of several novel alkenol analogs of 1-octen-3-ol as attractants to adult *Aedes albopictus*  
23 and *Culex quinquefasciatus*., *J. Am. Mosq. Control Assoc.*, 27(3), 256–262,  
24 doi:10.2987/10-6097.1, 2011.
- 25 Fischer, E. V., Jacob, D. J., Yantosca, R. M., Sulprizio, M. P., Millet, D. B., Mao, J.,  
26 Paulot, F., Singh, H. B., Roiger, A., Ries, L., Talbot, R. W., Dzepina, K. and Pandey  
27 Deolal, S.: Atmospheric peroxyacetyl nitrate (PAN): A global budget and source  
28 attribution, *Atmos. Chem. Phys.*, 14(5), 2679–2698, doi:10.5194/acp-14-2679-2014,  
29 2014.
- 30 Fu, T. M., Jacob, D. J., Wittrock, F., Burrows, J. P., Vrekoussis, M. and Henze, D. K.:  
31 Global budgets of atmospheric glyoxal and methylglyoxal, and implications for  
32 formation of secondary organic aerosols, *J. Geophys. Res. Atmos.*, 113, D15,  
33 doi:10.1029/2007JD009505, 2008.
- 34 Gaona-Colmán, E., Blanco, M. B. and Teruel, M. A.: Kinetics and product  
35 identification of the reactions of (*E*)-2-hexenyl acetate and 4-methyl-3-penten-2-one  
36 with OH radicals and Cl atoms at 298 K and atmospheric pressure, *Atmos. Environ.*,  
37 161, 155–166, doi:10.1016/j.atmosenv.2017.04.033, 2017.
- 38 Gøgsig, T. M., Nielsen, D. U., Lindhardt, A. T. and Skrydstrup, T.: Palladium catalyzed  
39 carbonylative Heck reaction affording monoprotected 1,3-ketoaldehydes, *Org. Lett.*,  
40 14(10), 2536–2539, doi:10.1021/ol300837d, 2012.
- 41 Green, M., Yarwood, G. and Niki, H.: FTIR study of the Cl-atom initiated oxidation of  
42 methylglyoxal, *Int. J. Chem. Kinet.*, 22(7), 689–699, doi:10.1002/kin.550220705, 1990.



- 1 Grosjean, E. and Grosjean, D.: The reaction of unsaturated aliphatic oxygenates with  
2 ozone, *J. Atmos. Chem.*, 32(2), 205–232, doi:10.1023/A:1006122000643, 1999.
- 3 Hatch, L. E., Luo, W., Pankow, J. F., Yokelson, R. J., Stockwell, C. E. and Barsanti, K.  
4 C.: Identification and quantification of gaseous organic compounds emitted from  
5 biomass burning using two-dimensional gas chromatography-time-of-flight mass  
6 spectrometry, *Atmos. Chem. Phys.*, 15(4), 1865–1899, doi:10.5194/acp-15-1865-2015,  
7 2015.
- 8 Holloway, A. L., Treacy, J., Sidebottom, H., Mellouki, A., Daële, V., Le Bras, G. and  
9 Barnes, I.: Rate coefficients for the reactions of OH radicals with the keto/enol  
10 tautomers of 2,4-pentanedione and 3-methyl-2,4-pentanedione, allyl alcohol and methyl  
11 vinyl ketone using the enols and methyl nitrite as photolytic sources of OH, *J.*  
12 *Photochem. Photobiol. A Chem.*, 176(1-3 SPEC. ISS.), 183–190,  
13 doi:10.1016/j.jphotochem.2005.08.031, 2005.
- 14 Jiménez, E., Cabañas, B. and Lefebvre, G.: Environment, Energy and Climate Change I,  
15 in *The Handbook of Environmental Chemistry*, Springer., 2014.
- 16 Kumar, N. R., Poornachandra, Y., Swaroop, D. K., Dev, G. J., Kumar, C. G. and  
17 Narsaiah, B.: Synthesis of novel ethyl 2,4-disubstituted 8-  
18 (trifluoromethyl)pyrido[2',3':3,4]pyrazolo[1,5-a]pyrimidine-9-carboxylate derivatives  
19 as promising anticancer agents., *Bioorg. Med. Chem. Lett.*, 26(21), 5203–5206, 2016.
- 20 Kung, J. T.: New caramel compound from coffee, *J. Agric. Food Chem.*, 22(3), 494–  
21 496, 1974.
- 22 Li, M., Liu, Y. and Wang, L.: Gas-phase ozonolysis of furans, methylfurans, and  
23 dimethylfurans in the atmosphere, *Phys. Chem. Chem. Phys.*, 20(38), 24735–24743,  
24 doi:10.1039/c8cp04947e, 2018.
- 25 Logan, J. A.: Tropospheric ozone: seasonal behavior, trends, and anthropogenic  
26 influence., *J. Geophys. Res.*, 90(D6), 10463–10482, doi:10.1029/JD090iD06p10463,  
27 1985.
- 28 Lv, C., Du, L., Tsona, N., Jiang, X. and Wang, W.: Atmospheric Chemistry of 2-  
29 Methoxypropene and 2-Ethoxypropene: Kinetics and Mechanism Study of Reactions  
30 with Ozone, *Atmosphere (Basel)*, 9(10), 401, 2018.
- 31 Mellouki, A., Le Bras, G. and Sidebottom, H.: Kinetics and Mechanisms of the  
32 Oxidation of Oxygenated Organic Compounds in the Gas Phase, *Chem. Rev.*, 103(12),  
33 5077–5096, doi:10.1021/cr020526x, 2003.
- 34 Mellouki, A., Wallington, T. J. and Chen, J.: Atmospheric Chemistry of Oxygenated  
35 Volatile Organic Compounds: Impacts on Air Quality and Climate, *Chem. Rev.*,  
36 115(10), 3984–4014, doi:10.1021/cr500549n, 2015.
- 37 Messaadia, L., El Dib, G., Ferhati, A. and Chakir, A.: UV-visible spectra and gas-phase  
38 rate coefficients for the reaction of 2,3-pentanedione and 2,4-pentanedione with OH  
39 radicals, *Chem. Phys. Lett.*, 626, 73–79, doi:10.1016/j.cplett.2015.02.032, 2015.
- 40 Szabó, E., Djehiche, M., Riva, M., Fittschen, C., Coddeville, P., Sarzyński, D., Tomas,  
41 A. and Dóbé, S.: Atmospheric chemistry of 2,3-pentanedione: Photolysis and reaction  
42 with OH radicals, *J. Phys. Chem. A*, 115(33), 9160–9168, doi:10.1021/jp205595c,



- 1 2011.
- 2 Taylor, O. C.: Importance of peroxyacetyl nitrate (pan) as a phytotoxic air pollutant, J.  
3 Air Pollut. Control Assoc., 19(5), 347–351, doi:10.1080/00022470.1969.10466498,  
4 1969.
- 5 Taylor, W. D., Allston, T. D., Moscato, M. J., Fazekas, G. B., Kozlowski, R. and  
6 Takacs, G. A.: Atmospheric photodissociation lifetimes for nitromethane, methyl nitrite,  
7 and methyl nitrate, Int. J. Chem. Kinet., 12(4), 231–240, doi:10.1002/kin.550120404,  
8 1980.
- 9 Tuazon, E. C., Leod, H. Mac, Atkinson, R. and Carter, W. P.:  $\alpha$ -Dicarbonyl Yields from  
10 the NO<sub>x</sub>-Air Photooxidations of a Series of Aromatic Hydrocarbons in Air, Environ.  
11 Sci. Technol., 20(4), 383–387, doi:10.1021/es00146a010, 1986.
- 12 US EPA. Estimation Programs Interface Suite™ for Microsoft® Windows, v 4. 11. E.  
13 P. A.: AOPWIN, 2018.
- 14 Vereecken, L., Aumont, B., Barnes, I., Bozzelli, J. W., Goldman, M. J., Green, W. H.,  
15 Madronich, S., McGillen, M. R., Mellouki, A., Orlando, J. J., Picquet-Varrault, B.,  
16 Rickard, A. R., Stockwell, W. R., Wallington, T. J. and Carter, W. P. L.: Perspective on  
17 Mechanism Development and Structure-Activity Relationships for Gas-Phase  
18 Atmospheric Chemistry, Int. J. Chem. Kinet., 50(6), 435–469, doi:10.1002/kin.21172,  
19 2018.
- 20 Villanueva, F., Cabañas, B., Monedero, E., Salgado, S., Bejan, I. and Martin, P.:  
21 Atmospheric degradation of alkylfurans with chlorine atoms: Product and mechanistic  
22 study, Atmos. Environ., 43(17), 2804–2813, doi:10.1016/j.atmosenv.2009.02.030, 2009.
- 23 Winiberg, F. A. F., Dillon, T. J., Orr, S. C., Groß, C. B. M., Bejan, I., Brumby, C. A.,  
24 Evans, M. J., Smith, S. C., Heard, D. E. and Seakins, P. W.: Direct measurements of  
25 OH and other product yields from the HO<sub>2</sub> + CH<sub>3</sub>C(O)O<sub>2</sub> reaction, Atmos. Chem.  
26 Phys., 16(6), 4023–4042, doi:10.5194/acp-16-4023-2016, 2016.
- 27 Zarzana, K. J., Selimovic, V., Koss, A. R., Sekimoto, K., Coggon, M. M., Yuan, B.,  
28 Dubé, W. P., Yokelson, R. J., Warneke, C., De Gouw, J. A., Roberts, J. M. and Brown,  
29 S. S.: Primary emissions of glyoxal and methylglyoxal from laboratory measurements  
30 of open biomass burning, Atmos. Chem. Phys., 18(20), 15451–15470, doi:10.5194/acp-  
31 18-15451-2018, 2018.
- 32 Zhou, S., Barnes, I., Zhu, T., Klotz, B., Albu, M., Bejan, I. and Benter, T.: Product  
33 study of the OH, NO<sub>3</sub>, and O<sub>3</sub> initiated atmospheric photooxidation of propyl vinyl  
34 ether, Environ. Sci. Technol., 40(17), 5415–5421, doi:10.1021/es0605422, 2006.
- 35 Zhou, S., Barnes, I., Zhu, T., Bejan, I., Albu, M. and Benter, T.: Atmospheric chemistry  
36 of acetylacetone, Environ. Sci. Technol., 42(21), 7905–7910, doi:10.1021/es8010282,  
37 2008.

38

39

40



1  
2  
3  
4



1 **Figure Captions**

2 **Figure 1:** Relative rate data for the reaction of OH radicals with (*E*)-4-methoxy-3-buten-2-one  
3 using propene (■) and isobutene (●) as reference compounds at 298 K and atmospheric pressure  
4 of air.

5

6 **Figure 2:** Relative rate data for the reaction of OH radicals with 1-(*E*)-1-methoxy-2-methyl-1-  
7 penten-3-one using propene (■) and isobutene (●) as reference compounds at 298 K and  
8 atmospheric pressure of air.

9

10 **Figure 3:** Infrared spectral data: trace A infrared spectrum of a TMBO/CH<sub>3</sub>ONO/NO/air reaction  
11 mixture before irradiation; trace B mixture after 10 min irradiation; trace C reference spectrum of  
12 TMBO; trace D product spectrum; trace E reference spectrum of methyl formate; trace F reference  
13 spectrum of peroxyacetyl nitrate; trace G reference spectrum of methyl glyoxal; trace H residual  
14 spectrum after subtraction of the identified reaction products in trace D.

15 **Figure 4:** Concentration–time dependencies for the reaction of TMBO (■) + OH radicals and  
16 the quantified products, methyl formate (◆MF), peroxyacetyl nitrate (●PAN), and methyl glyoxal  
17 (▲MG).

18 **Figure 5:** Infrared spectral data: trace A infrared spectrum of a MMPO/CH<sub>3</sub>ONO/NO/air reaction  
19 mixture before irradiation; trace B mixture after 10 min irradiation; trace C reference spectrum of  
20 MMPO; traced product spectrum; trace E reference spectrum of methyl formate; trace F reference  
21 spectrum of 2, 3-pentanedione; trace G reference spectrum of PPN; trace H residual spectrum  
22 after subtraction of the identified reaction products in trace D.

23 **Figure 6:** Concentration–time profiles for the reaction of 1-(*E*)-1-methoxy-2-methyl-1-  
24 penten-3-one (■MMPO) + OH radicals and the quantified product methyl formate (◆MF)  
25 and peroxypropionyl nitrate (●PPN).

26

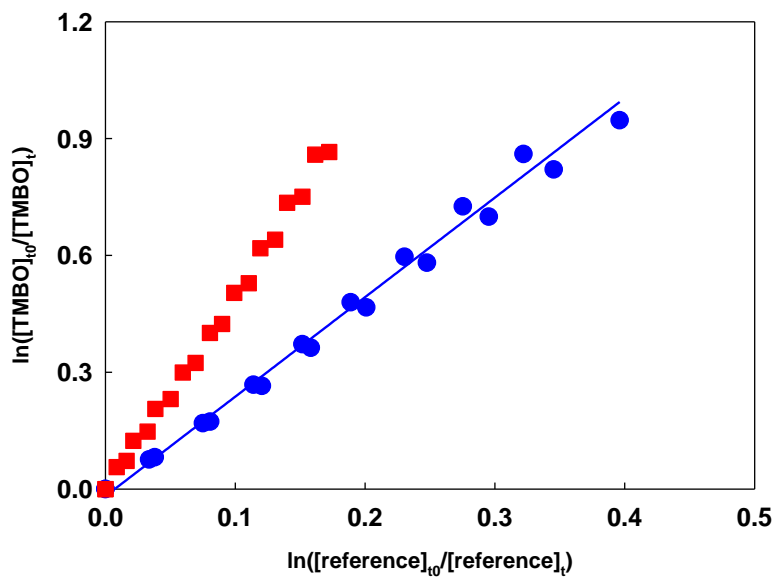
27

28



1

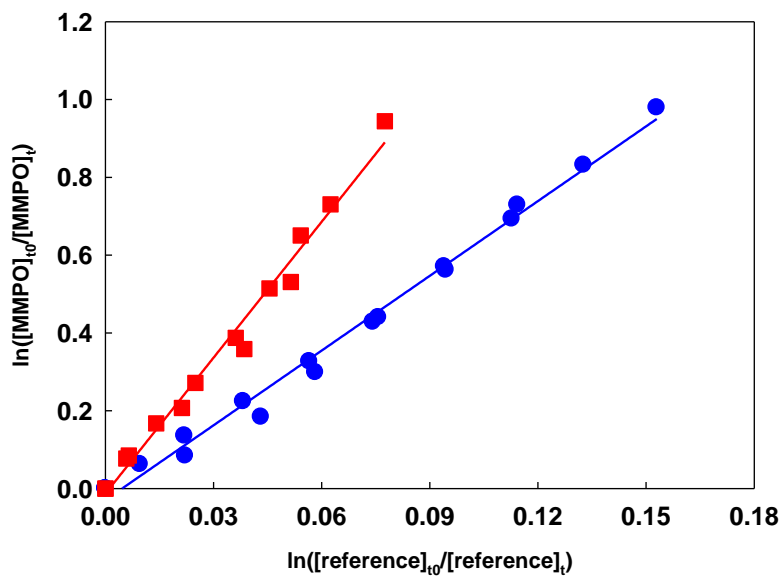
Fig. 1



2

3

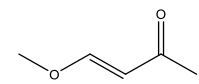
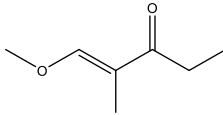
Fig.2



4



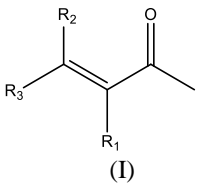
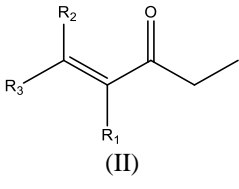
1 **Table 1.** Rate coefficient ratios  $k_{UKE}/k_{Reference}$  and rate coefficients for the reaction of OH radicals  
2 with (*E*)-4-methoxy-3-buten-2-one and (*E*)-1-methoxy-2-methyl-1-penten-3-one at ( $298 \pm 3$ ) K in  
3 1 atm of air.  
4

| Compound   | Reference      | $k_{UKE}/k_{Reference}$ | $k_{UKE+OH}$ ( $10^{-10}\text{cm}^3$<br>molecule $^{-1}\text{s}^{-1}$ ) |
|--|----------------|-------------------------|---|
| <br>Trans-4-Methoxy-3-buten-2-one                   | Isobutene      | ( $2.41 \pm 0.02$ )     | ( $1.26 \pm 0.06$ )   |
|  | Isobutene      | ( $2.74 \pm 0.04$ )     | ( $1.43 \pm 0.07$ )   |
|  | Propene        | ( $5.02 \pm 0.06$ )     | ( $1.46 \pm 0.05$ )   |
|  | Propene        | ( $5.20 \pm 0.07$ )     | ( $1.51 \pm 0.06$ )   |
|  | <b>Average</b> |                         | <b>(<math>1.42 \pm 0.12</math>)</b>                                     |
| <br>( <i>E</i> )-1-methoxy-2-methyl-1-penten-3-one | Isobutene      | ( $6.30 \pm 0.12$ )     | ( $3.30 \pm 0.16$ )   |
|  | Isobutene      | ( $6.54 \pm 0.38$ )     | ( $3.42 \pm 0.25$ )   |
|  | Propene        | ( $11.00 \pm 0.77$ )    | ( $3.19 \pm 0.25$ )   |
|  | Propene        | ( $11.88 \pm 0.49$ )    | ( $3.45 \pm 0.19$ )   |
|  | <b>Average</b> |                         | <b>(<math>3.34 \pm 0.43</math>)</b>                                     |

5  
6  
7  
8  
9  
10  
11  
12  
13  
14  
15  
16  
17  
18  
19  
20  
21  
22  
23  
24  
25  
26  
27



1 **Table 2.** OH rate coefficients for different unsaturated ketones obtained experimentally  
 2 and predicted using a SAR method.  
 3

| Basic structure   | Substituent -R               | Compound name                         | Experimental $k_{OH}(\text{cm}^3 \text{ molecule}^{-1} \text{ s}^{-1})$ | SAR calculated $k_{OH}^f(\text{cm}^3 \text{ molecule}^{-1} \text{ s}^{-1})$   |
|---|------------------------------|---------------------------------------|---|---|
|  <p>(I)</p>    | $R_1=R_2=R_3=H$              | 3-buten-2-one                         | $(2.0 \pm 0.3) \times 10^{-11a}$  | $H_{\text{abs}}=1.02 \times 10^{-13}$<br>$OH_{\text{Add}}=2.37 \times 10^{-11}$<br><b>Overall= <math>2.38 \times 10^{-11}</math></b>                        |
|   | $R_1=H, R_2=H, R_3=CH_3$     | 3-penten-2-one                        | $(7.22 \pm 1.74) \times 10^{-11b}$                                      | <i>Trans-isomer</i><br>$H_{\text{abs}}=2.38 \times 10^{-13}$<br>$OH_{\text{Add}}=5.76 \times 10^{-11}$<br><b>Overall= <math>5.78 \times 10^{-11}</math></b> |
|   | $R_1=H, R_2=CH_3, R_3=CH_3$  | 4-methyl-3-penten-2-one               | $(1.02 \pm 0.20) \times 10^{-10c}$                                      | $H_{\text{abs}}=3.74 \times 10^{-13}$<br>$OH_{\text{Add}}=7.82 \times 10^{-11}$<br><b>Overall= <math>7.86 \times 10^{-11}</math></b>                        |
|   | $R_1=H, R_2=H, R_3=OCH_3$    | (E)-4-methoxy-3-buten-2-one           | $(1.42 \pm 0.12) \times 10^{-10d}$                                      | $H_{\text{abs}}=9.32 \times 10^{-13}$<br>$OH_{\text{Add}}=7.49 \times 10^{-11}$<br><b>Overall= <math>7.58 \times 10^{-11}</math></b>                        |
|  <p>(II)</p> | $R_1=R_2=R_3=H$              | 1-penten-3-one                        | $(2.90 \pm 0.79) \times 10^{-11e}$                                      | $H_{\text{abs}}=1.23 \times 10^{-12}$<br>$OH_{\text{Add}}=2.37 \times 10^{-11}$<br><b>Overall= <math>2.49 \times 10^{-11}</math></b>                        |
|   | $R_1=H, R_2=H, R_3=CH_3$     | (E)-4-hexen-3-one                     | $(9.04 \pm 2.12) \times 10^{-11b}$                                      | <i>Trans-isomer</i><br>$H_{\text{abs}}=1.37 \times 10^{-12}$<br>$OH_{\text{Add}}=5.76 \times 10^{-11}$<br><b>Overall= <math>5.90 \times 10^{-11}</math></b> |
|   | $R_1=H, R_2=CH_3, R_3=CH_3$  | 5-methyl-4-hexen-3-one                | -   | $H_{\text{abs}}=1.50 \times 10^{-12}$<br>$OH_{\text{Add}}=7.82 \times 10^{-11}$<br><b>Overall= <math>7.97 \times 10^{-11}</math></b>                        |
|   | $R_1=CH_3, R_2=H, R_3=OCH_3$ | (E)-1-methoxy-2-methyl-1-penten-3-one | $(3.34 \pm 0.43) \times 10^{-10d}$                                      | $H_{\text{abs}}=2.20 \times 10^{-12}$<br>$OH_{\text{Add}}=1.02 \times 10^{-10}$<br><b>Overall= <math>1.04 \times 10^{-10}</math></b>                        |

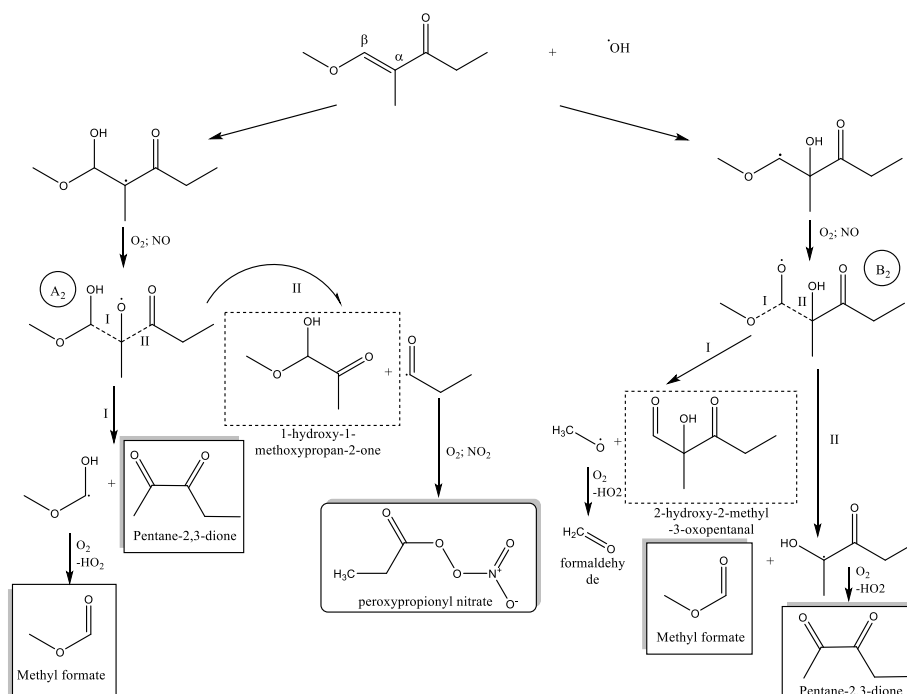
4 a-(Holloway et al., 2005)  
 5 b-(Blanco et al., 2012)  
 6 c-(Gaona-Colmán et al., 2017)  
 7 d- This work  
 8 e-(Blanco and Teruel, 2011)

9  
 10  
 11  
 12





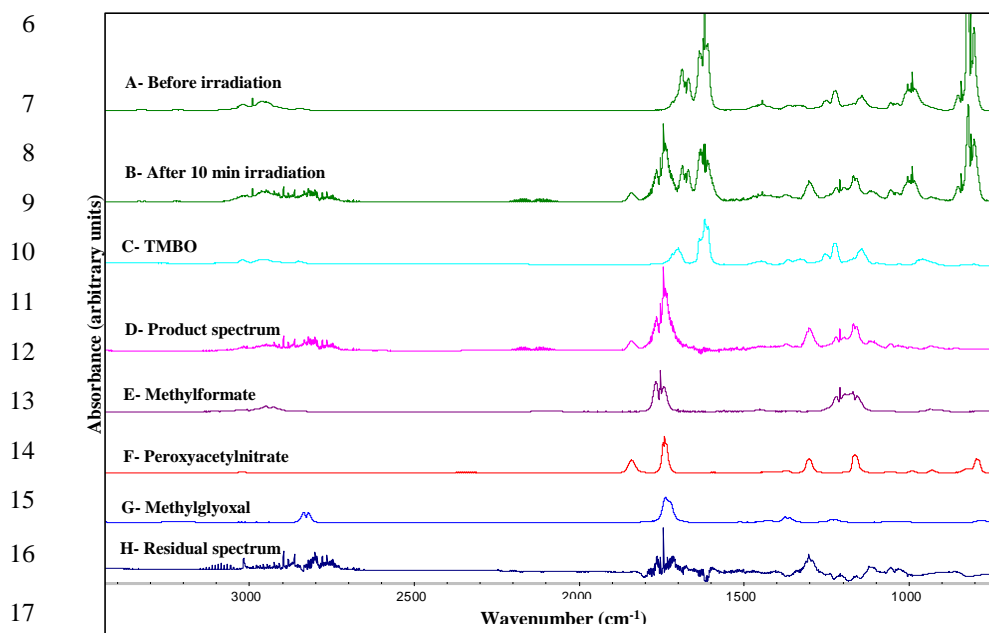
1 **Scheme 2.** Simplified reaction mechanism for the addition channel in the OH-radical  
 2 initiated oxidation of 1-(*E*)-1-methoxy-2-methyl-1-penten-3-one.  
 3



4

5

Fig. 3

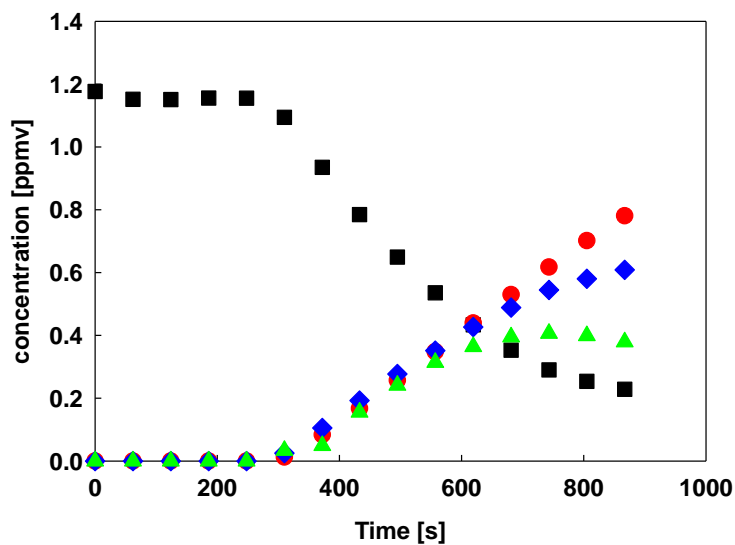


17



1

Fig. 4

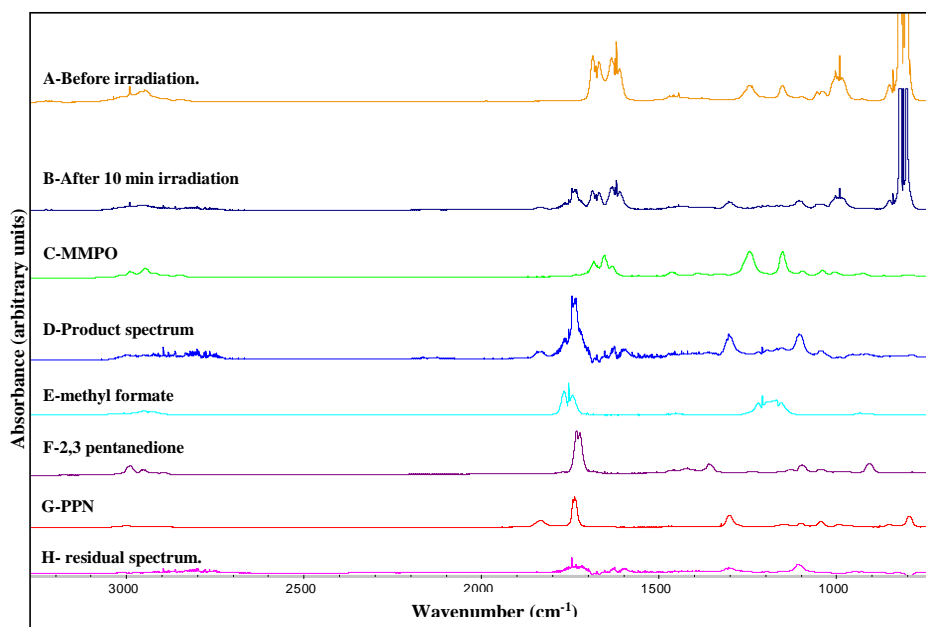


2

3

4

Fig. 5



5

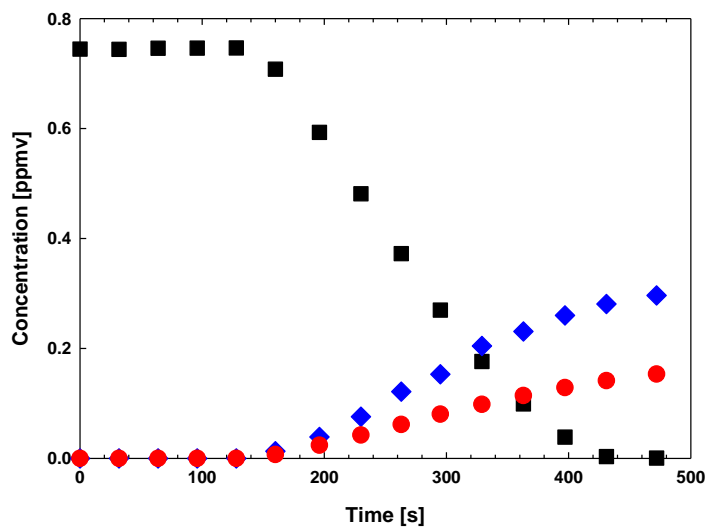
6

7



1

Fig. 6



2  
3  
4  
5  
6